

Upper critical field and quantum oscillations in tetragonal superconducting FeS

Taichi Terashima,¹ Naoki Kikugawa,¹ Hai Lin,² Xiyu Zhu,² Hai-Hu Wen,²
Takuya Nomoto,³ Katsuhiko Suzuki,⁴ Hiroaki Ikeda,⁵ and Shinya Uji¹

¹*National Institute for Materials Science, Tsukuba, Ibaraki 305-0003, Japan*

²*Center for Superconducting Physics and Materials,*

*National Laboratory of Solid State Microstructures and Department of Physics,
National Center of Microstructures and Quantum Manipulation, Nanjing University, Nanjing 210093, China*

³*Department of Physics, Kyoto University, Kyoto, 606-8502, Japan*

⁴*Research Organization of Science and Technology,*

Ritsumeikan University, Kusatsu, Shiga 525-8577, Japan

⁵*Department of Physics, Ritsumeikan University, Kusatsu, Shiga 525-8577, Japan*

(Dated: July 19, 2022)

Magnetoresistance and magnetic torque are measured on FeS down to 0.03 K in magnetic fields B up to 18 T. The superconducting transition temperature is $T_c = 4.1$ K, and the anisotropy ratio of the upper critical field B_{c2} at T_c is estimated from the initial slopes to be $\Gamma(T_c) = 6.9$. $B_{c2}(0)$ is estimated to be 2.2 and 0.36 T for $B \parallel ab$ and c , respectively. Quantum oscillations are observed in both resistance and torque. Two frequencies $F = 0.15$ and 0.20 kT are resolved and assigned to a quasi-two-dimensional Fermi surface cylinder. The carrier density and Sommerfeld coefficient associated with this cylinder are estimated to be 5.8×10^{-3} carriers/Fe and 0.48 mJ/(K²mol). There remain other Fermi surface pockets still to be found. Band-structure calculations are performed and compared to the experimental results.

PACS numbers: 74.70.Xa, 74.25.Dw, 74.25.Jb, 71.18.+y

Since the discovery of superconductivity (SC) at $T_c = 26$ K in LaFeAs(O_{1-x}F_x) by Kamihara *et al.* [1], layered iron pnictides and chalcogenides have been studied extensively. Very recently, an interesting new member has joined the group: tetragonal FeS with the same PbO-type structure as FeSe [2]. Instead of previous synthesis routes, which failed, Lai *et al.* used a hydrothermal method and obtained highly stoichiometric tetragonal FeS crystals showing superconductivity below $T_c \approx 5$ K. This has aroused considerable interest and initiated researches into superconducting properties of FeS [3–9]: A nodal or highly-anisotropic superconducting gap has been suggested by a specific-heat [6] or a scanning-tunneling-microscopy study [9], while a μ SR study suggests a full-gap state coexisting with low-moment disordered magnetism [7]. A large anisotropy of the upper critical field B_{c2} has been reported [4, 8].

Not to mention that studies on FeS are important in themselves, comparative studies of FeS and the sister compound FeSe will also be particularly helpful in uncovering origins of the peculiarities of FeSe. FeSe ($T_c \approx 8$ K [10]) exhibits a tetragonal-to-orthorhombic transition, but no accompanying magnetic order occurs at ambient pressure [11], unlike typical iron pnictide parent compounds such as LaFeAsO or BaFe₂As₂ [12, 13]. Application of pressure not only enhances T_c remarkably to 37 K (onset) [14, 15] but also induces an antiferromagnetic order [16–18]. The electronic structure is markedly different from that predicted by band-structure calculations: the Fermi surface (FS) is anomalously small

[19–23] and a large splitting of the Fe $3d_{xz}$ and d_{yz} bands have been reported [24–26]. The smallness of the Fermi energy E_F relative to T_c suggests that physics of the Bardeen-Cooper-Schrieffer (BCS)–Bose-Einstein-condensation (BEC) crossover may be relevant to superconducting properties of FeSe [27–29].

In this paper, we report magnetoresistance and magnetic torque measurements on FeS crystals. The upper critical field B_{c2} is determined from the magnetoresistance data down to 0.03 K for magnetic fields B parallel to the c axis and the ab plane. Quantum oscillations are observed in both the magnetoresistance and the magnetic torque at high fields. Results are discussed in light of band-structure calculations.

Tetragonal FeS single crystals were prepared by a hydrothermal method as described in Ref. [8]. For four-contact in-plane resistance measurements, electrical contacts were attached to four samples with silver paste first, but only one could be measured down to low temperatures. As the contacts changed color to black, it seemed that the contacts were degraded by formation of AgS. Then, carbon paste was used for another three samples, two of which could be measured at low temperatures. Typical sample dimensions of the resistance samples are roughly $0.7 \times 0.2 \times 0.02$ mm³. The resistance ratio between room temperature and 4.5 K is 14–25. Magnetic torque was measured on four samples with typical dimensions of $0.2 \times 0.2 \times 0.02$ mm³ using piezoresistive microcantilevers [30]. A dilution refrigerator and a superconducting magnet were used to generate low tem-

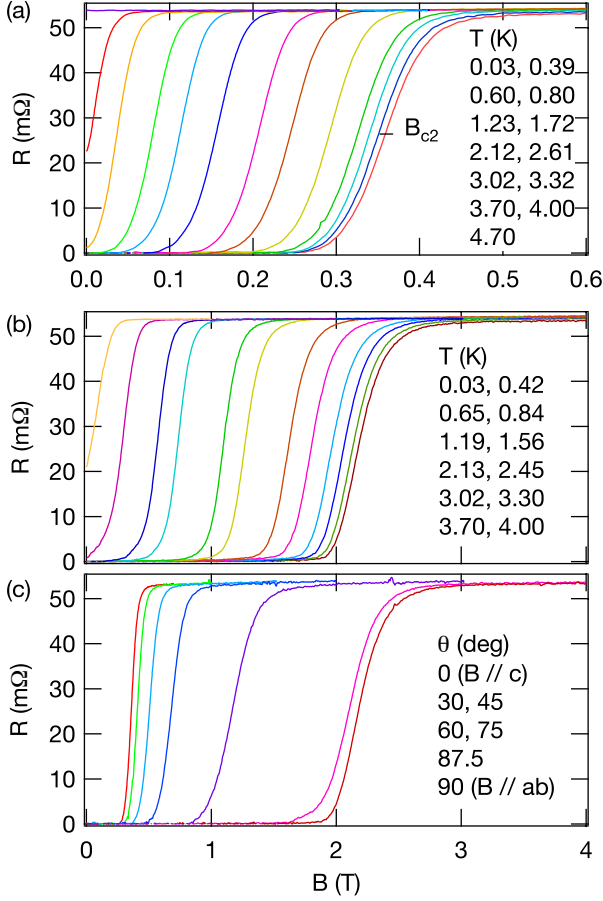


FIG. 1. (Color online). (a) and (b) In-plane resistance R in FeS as a function of magnetic field B parallel to the c axis (a) and the ab plane (b) for selected temperatures. B_{c2} is defined with a midpoint criterion as indicated in (a). (c) R vs B for selected field directions. $T \leq 0.04$ K.

peratures down to $T = 0.03$ K and high magnetic fields up to $B = 17.8$ T. The magnetic field direction θ is measured from the c axis. Relativistic electronic structure calculations were performed by using the WIEN2K code [31] with the experimental lattice parameters [2, 32]

Figure 1 shows resistive transition curves for $B \parallel c$ (a) and $B \parallel ab$ (b) for selected temperatures as well as for selected field directions (c) for $T \leq 0.04$ K. We define B_{c2} by a midpoint criterion as indicated in (a). Figure 2(a) shows B_{c2} as a function of temperature for $B \parallel ab$ and $B \parallel c$. The initial slopes $dB_{c2}/dT|_{T_c}$ for $B \parallel ab$ and $B \parallel c$ are estimated from linear fits to data points for $T \geq 3.3$ K (solid lines) to be -0.75 and -0.11 T/K, respectively, the ratio of which gives the anisotropy ratio $\Gamma(T_c) = 6.9$. The coherence length ξ can be estimated to be 33 and 4.7 nm for $\parallel ab$ and $\parallel c$, respectively. The intercepts of the fitted lines give $T_c = 4.1$ K. The upper critical field as $T \rightarrow 0$ is $B_{c2}(0) = 2.2$ and 0.36 T for $B \parallel ab$ and $B \parallel c$, respectively, giving $\Gamma(0) = 6.1$. In the case of FeSe, B_{c2}

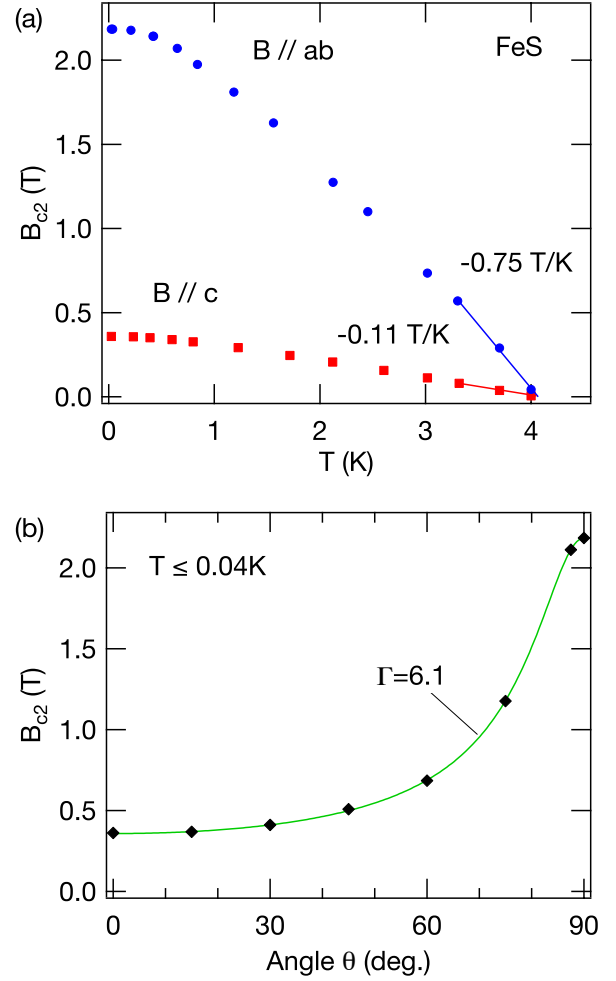


FIG. 2. (Color online). (a) Temperature dependence of B_{c2} for $B \parallel ab$ and $B \parallel c$. (b) Angle dependence of B_{c2} . The solid curve is calculated with an anisotropic Ginzburg-Landau model.

for $B \parallel ab$ is anomalously enhanced at lowest temperatures below ~ 1 K [20], while no such enhancement is observed in FeS. An anisotropic Ginzburg-Landau model with $\Gamma(0) = 6.1$ explains the angle dependence of the upper critical field measured at $T \leq 0.04$ K perfectly as shown in Fig. 2(b). These superconducting parameters are in good agreement with [8]. On the other hand, the anisotropy ratio of $\Gamma \sim 10$ reported in [4] is significantly larger than our value. This might be related to the fact that T_c of a resistivity sample in [4] is rather lower than our T_c : it has been reported that $T_c^{\text{onset}} = 3.5$ K and that $T_c^{\text{zero}} = 2.4$ K.

It is interesting to compare superconducting parameters between FeS and FeSe. The initial slopes in FeSe are much larger [20]: $dB_{c2}/dT|_{T_c} = -6.9$ and -1.6 T/K for $B \parallel ab$ and $B \parallel c$, respectively, which are factors of 9.1 and 15 larger than the corresponding values in FeS. Within a single-band BCS theory, $dB_{c2}/dT|_{T_c} \sim \gamma^2 T_c / S^2$, where

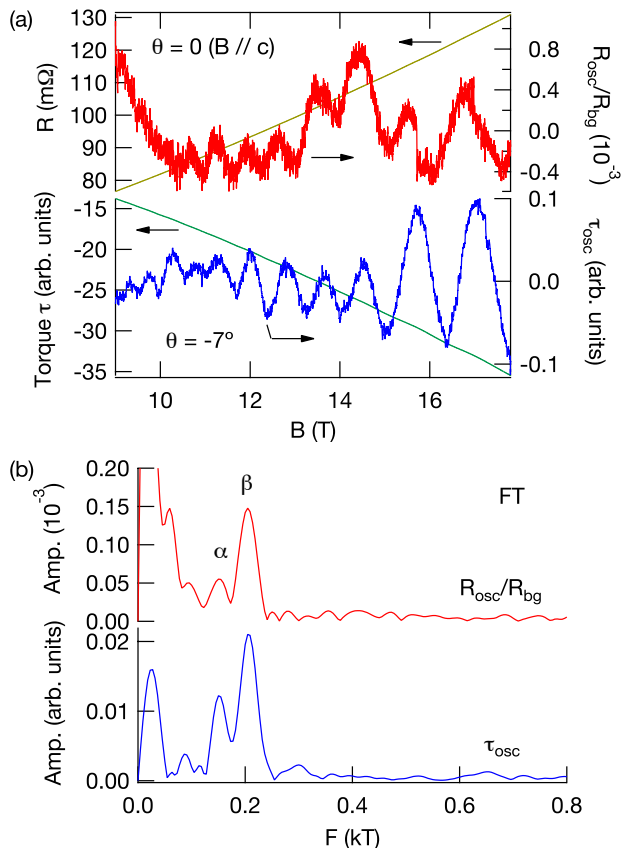


FIG. 3. (Color online). (a) Magnetoresistance in FeS for $B \parallel c$ at $T = 0.11$ K (upper curve) and magnetic torque for $\theta = -7^\circ$ at $T = 0.07$ K (lower) as a function of magnetic field. Their oscillatory parts are also shown (right axis). (b) Fourier transform amplitudes of the oscillations in $1/B$.

S is the surface area of the FS [33]. To evaluate the right-hand side of the relation, we use the Sommerfeld coefficient of $\gamma = 5.73$ mJ/(mol K²) [34] and $T_c = 9.1$ K for FeSe [20]. For FeS, $\gamma = 3.8$ mJ/(mol K²) [6], and, since T_c for FeSe was determined with a zero-resistance criterion in [20], we use a similarly determined T_c of 3.9 K for FeS for the comparison. The ratio of $\gamma^2 T_c / S^2$ between FeSe and FeS is evaluated to be $5.2(S_{FeS} / S_{FeSe})^2$. The experimental ratio of 9.1 or 15 suggests $(S_{FeS} / S_{FeSe}) = 1.3$ or 1.7, which may suggest that FeS has a larger FS and hence a larger carrier density. Secondly, the anisotropy ratio $\Gamma(T_c) = 6.9$ is larger than the ratio of 4.3 in FeSe. Since $\Gamma^2 = m_c / m_{ab}$, where $m_{c(ab)}$ is the effective mass along the c (ab) direction, this suggests that FeS has a more two-dimensional electronic structure, i.e., smaller dispersion along the c axis.

Owing to the high quality of the crystals, the magnetoresistance exhibits Shubnikov–de Haas (SdH) oscillations at high fields. Figure 3(a) shows an $R(B)$ curve for $B \parallel c$ (upper curve). After subtracting a smooth background modeled by a second-order polynomial, clear os-

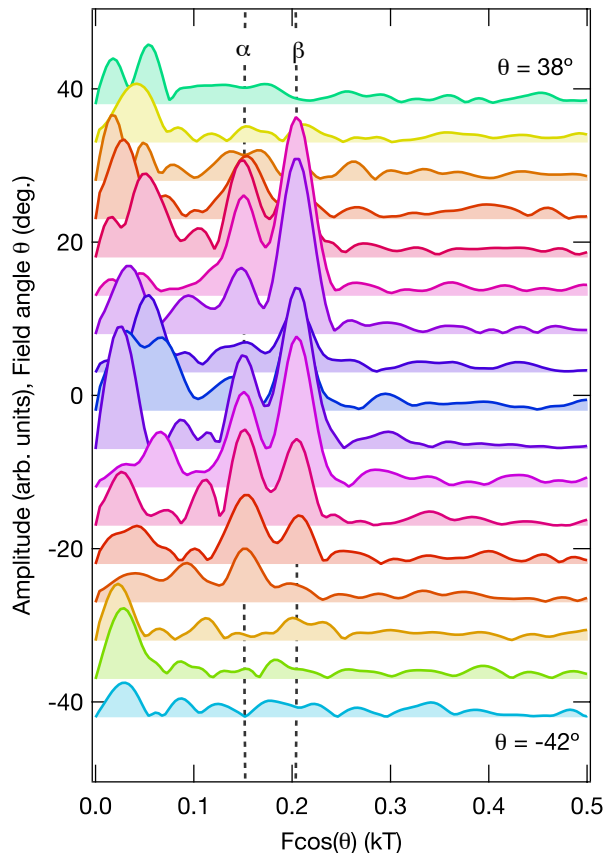


FIG. 4. (Color online). Fourier transform amplitudes of torque dHvA oscillations in FeS for different field directions. Note that the horizontal axis is $F \cos \theta$. Spectra are shifted vertically so that the baseline of a spectrum for the angle θ is placed at θ . The dotted lines indicate the θ -variation of $F \cos \theta$ calculated with the Yamaji model of a quasi-two-dimensional FS cylinder (see text).

illations appear. The corresponding Fourier spectrum shows two peaks marked by α and β [Fig. 3(b), upper curve].

To further study the FS in FeS, we also tried magnetic torque measurements. The lower part of Fig. 3(a) shows the magnetic torque at $\theta = -7^\circ$ and its oscillatory part, i.e., de Haas–van Alphen (dHvA) oscillations, as a function of B . The smooth background was modeled by a third-order polynomial. The corresponding Fourier spectrum [Fig. 3(b), lower curve] shows the α and β frequencies consistent with the SdH data. Figure 4 shows angular variation of Fourier spectra. Note that the horizontal axis is $F \cos \theta$. The symmetric appearance of the frequency peaks with respect to $\theta = 0$ and the suppressed oscillation amplitudes near $\theta = 0$ conform to the crystal symmetry of FeS.

All of the three resistance and four torque samples exhibit quantum oscillations with the α and β frequencies, demonstrating that the two frequencies are intrinsic to

tetragonal FeS. The effective masses associated with the two frequencies are estimated from the temperature dependence of the oscillation amplitudes as usual [35]. Averaged over four samples with larger oscillation amplitudes, the frequencies and effective masses for $B \parallel c$ are estimated as follows: $F_\alpha = 153(2)$ T, $m_\alpha^*/m_e = 0.62(3)$, $F_\beta = 203.5(2)$ T, and $m_\beta^*/m_e = 0.83(1)$, where m_e is the free-electron mass. The frequencies correspond to the orbit areas occupying only 0.50 and 0.67% of the Brillouin zone. The effective Fermi energy can be calculated to be $E_F = 28$ meV for both orbits, which is larger than E_F values found in FeSe and suggests that FeS is not close to the BCS-BEC crossover. The electron mean free path l can be estimated only very roughly because of the small number of observed oscillation periods: $l \approx 40\text{--}80$ nm for the β orbit, which is comparable or slightly larger than the in-plane coherence length.

We assign the two frequencies to the minimum and maximum cross sections of a quasi-two-dimensional FS cylinder. Yamaji previously considered a quasi-two-dimensional FS cylinder with a cosine energy dispersion along the c axis [36]. The dotted lines in Fig. 4 show the angle dependence of $F \cos \theta$ of the two frequencies expected from the Yamaji model. The observed frequency peaks are consistent with the calculated lines, supporting the assignment. The two dimensionality of an FS cylinder may be judged from $\Delta F/F_{av}$, where ΔF and F_{av} are the difference and average of the minimum and maximum frequencies: this parameter is 0.28 for the present FS cylinder in FeS, while it is larger than 1 for experimentally observed FS cylinders in FeSe [20]. This suggests that FeS is more two dimensional in the electronic structure and consistent with the larger B_{c2} anisotropy. The carrier density and Sommerfeld coefficient associated with the observed FS cylinder are estimated to be 5.8×10^{-3} carriers/Fe and 0.48 mJ/(K²mol). Since the experimental Sommerfeld coefficient is $\gamma_{exp} = 3.8$ mJ/(K²mol) [6], large parts of the FS still remain to be observed in future measurements.

Figure 5(a) shows the calculated band structure. The calculated Fermi surface (b) consists of two hole and two electron FS cylinders at the zone center and corner, respectively. The band structure and Fermi surface are in good agreement with [5], but not with [37], which suggested the third closed hole pocket at Γ . The discrepancy can be attributed to the difference in the atomic position z_S of S: while the experimental value of $z_S = 0.2523$ [2] was used in the present work and [5], the relaxed value of $z_S = 0.2243$ in [37]. The carrier density and Sommerfeld coefficient are estimated to be $n_e = n_h = 0.185$ carriers/Fe and $\gamma_{band} = 2.4$ mJ/(K²mol). The carrier density is slightly larger than that in FeSe (0.17 carriers/Fe) [20]. The latter gives the mass enhancement of $\gamma_{exp}/\gamma_{band} = 1 + \lambda = 1.6$. Clearly, the calculated FS cylinders are much larger than the experimentally observed one: the calculated quantum oscillation frequen-

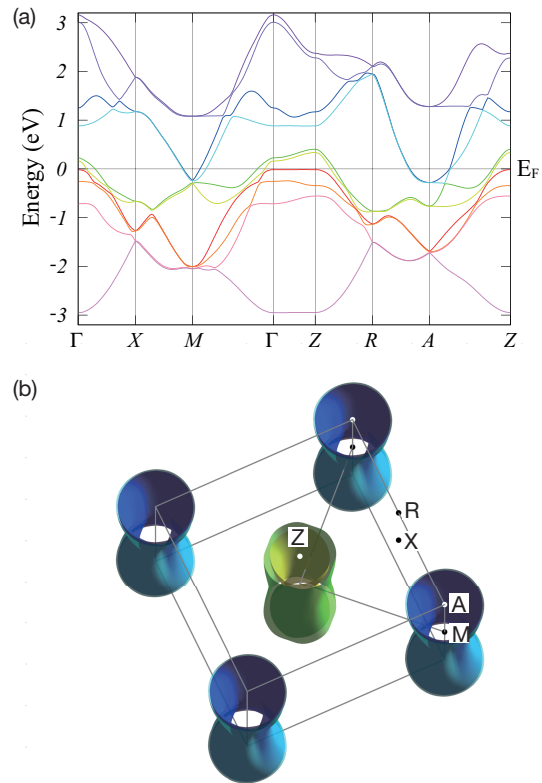


FIG. 5. (Color online). Calculated electronic band structure (a) and Fermi surface (b) in FeS.

cies are in a range between $F = 0.5$ and ~ 3 kT. This might indicate the FS shrinking: the experimentally observed FS's in FeSe and iron pnictides are smaller than predicted by band-structure calculations [20, 38–44]. Alternatively, the observed FS cylinder might be attributed to the third hole band, which is a nearly flat band sitting just below E_F along the ΓZ section. If this band is slightly raised up, there will be a fairly two-dimensional FS cylinder. Indeed, the corresponding band sits above E_F in a calculated band structure of FeSe [20].

In summary, we have performed magnetoresistance measurements on FeS down to 0.03 K and determined the upper critical field: $B_{c2}(0) = 2.2$ and 0.36 T for $B \parallel ab$ and c , respectively. The anisotropy ratio at T_c is $\Gamma(T_c) = 6.9$, which is consistent with [8]. We have observed quantum oscillations in both magnetoresistance and magnetic torque. Two frequencies $F = 0.15$ and 0.20 kT are resolved and attributed to a quasi-two-dimensional FS cylinder. The associated carrier density and Sommerfeld coefficient are estimated to be 5.8×10^{-3} carriers/Fe and 0.48 mJ/(K²mol). Band-structure calculations predict FS cylinder that are much larger than the observed one. It is a very important future magnetic task to find remaining FS cylinders using higher magnetic fields to judge how successful the calculations are.

This work was supported by JSPS KAKENHI Grant Numbers JP26400373, 15H05745, 15H02014, 16H01081, 16H04021, and 15J01476. The work in Nanjing University is supported by National Natural Science Foundation of China (NSFC) with the projects: A0402/11534005, A0402/11190023; the Ministry of Science and Technology of China (Grant No. 2016YFA0300404, 2012CB821403).

-
- [1] Y. Kamihara, T. Watanabe, M. Hirano, and H. Hosono, *J. Am. Chem. Soc.* **130**, 3296 (2008).
- [2] X. Lai, H. Zhang, Y. Wang, X. Wang, X. Zhang, J. Lin, and F. Huang, *J. Am. Chem. Soc.* **137**, 10148 (2015).
- [3] U. Pachmayr, N. Fehn, and D. Johrendt, *Chem. Commun.* **52**, 194 (2016).
- [4] C. K. H. Borg, X. Zhou, C. Eckberg, D. J. Campbell, S. R. Saha, J. Paglione, and E. E. Rodriguez, *Phys. Rev. B* **93**, 094522 (2016).
- [5] Y. Yang, W.-S. Wang, H.-Y. Lu, Y.-Y. Xiang, and Q.-H. Wang, *Phys. Rev. B* **93**, 104514 (2016).
- [6] J. Xing, H. Lin, Y. Li, S. Li, X. Zhu, H. Yang, and H.-H. Wen, *Phys. Rev. B* **93**, 104520 (2016).
- [7] S. Hohenstein, U. Pachmayr, Z. Guguchia, S. Kamusella, R. Khasanov, A. Amato, C. Baines, H.-H. Klauss, E. Morenzoni, D. Johrendt, and H. Luetkens, *Phys. Rev. B* **93**, 140506 (2016).
- [8] H. Lin, Y. Li, Q. Deng, J. Xing, J. Liu, X. Zhu, H. Yang, and H.-H. Wen, *Phys. Rev. B* **93**, 144505 (2016).
- [9] X. Yang, Z. Du, G. Du, Q. Gu, H. Lin, D. Fang, H. Yang, X. Zhu, and H.-H. Wen, *Phys. Rev. B* **94**, 024521 (2016).
- [10] F.-C. Hsu, J.-Y. Luo, K.-W. Yeh, T.-K. Chen, T.-W. Huang, P. M. Wu, Y.-C. Lee, Y.-L. Huang, Y.-Y. Chu, D.-C. Yan, and M.-K. Wu, *Proc. Nat. Acad. Sci. U. S. A.* **105**, 14262 (2008).
- [11] T. M. McQueen, A. J. Williams, P. W. Stephens, J. Tao, Y. Zhu, V. Ksenofontov, F. Casper, C. Felser, and R. J. Cava, *Phys. Rev. Lett.* **103**, 057002 (2009).
- [12] M. Rotter, M. Tegel, and D. Johrendt, *Phys. Rev. Lett.* **101**, 107006 (2008).
- [13] K. Sasmal, B. Lv, B. Lorenz, A. M. Guloy, F. Chen, Y.-Y. Xue, and C.-W. Chu, *Phys. Rev. Lett.* **101**, 107007 (2008).
- [14] Y. Mizuguchi, F. Tomioka, S. Tsuda, T. Yamaguchi, and Y. Takano, *Appl. Phys. Lett.* **93**, 152505 (2008).
- [15] S. Medvedev, T. M. McQueen, I. A. Troyan, T. Palasyuk, M. I. Erements, R. J. Cava, S. Naghavi, F. Casper, V. Ksenofontov, G. Wortmann, and C. Felser, *Nat. Mater.* **8**, 630 (2009).
- [16] M. Bendele, A. Amato, K. Conder, M. Elender, H. Keller, H.-H. Klauss, H. Luetkens, E. Pomjakushina, A. Raselli, and R. Khasanov, *Phys. Rev. Lett.* **104**, 087003 (2010).
- [17] M. Bendele, A. Ichsanow, Y. Pashkevich, L. Keller, T. Strässle, A. Gusev, E. Pomjakushina, K. Conder, R. Khasanov, and H. Keller, *Phys. Rev. B* **85**, 064517 (2012).
- [18] T. Terashima, N. Kikugawa, S. Kasahara, T. Watashige, T. Shibauchi, Y. Matsuda, T. Wolf, A. E. Böhmer, F. Hardy, C. Meingast, H. v. Löhneysen, and S. Uji, *J. Phys. Soc. Jpn.* **84**, 063701 (2015).
- [19] J. Maletz, V. B. Zabolotnyy, D. V. Evtushinsky, S. Thirupathiah, A. U. B. Wolter, L. Harnagea, A. N. Yaresko, A. N. Vasiliev, D. A. Chareev, A. E. Böhmer, F. Hardy, T. Wolf, C. Meingast, E. D. L. Rienks, B. Büchner, and S. V. Borisenko, *Phys. Rev. B* **89**, 220506 (2014).
- [20] T. Terashima, N. Kikugawa, A. Kiswandhi, E.-S. Choi, J. S. Brooks, S. Kasahara, T. Watashige, H. Ikeda, T. Shibauchi, Y. Matsuda, T. Wolf, A. E. Böhmer, F. Hardy, C. Meingast, H. v. Löhneysen, M.-T. Suzuki, R. Arita, and S. Uji, *Phys. Rev. B* **90**, 144517 (2014).
- [21] A. Audouard, F. Duc, L. Drigo, P. Toulemonde, S. Karlsson, P. Strobel, and A. Sulpice, *EPL (Europhysics Letters)* **109**, 27003 (2015).
- [22] M. D. Watson, T. K. Kim, A. A. Haghighirad, N. R. Davies, A. McCollam, A. Narayanan, S. F. Blake, Y. L. Chen, S. Ghannadzadeh, A. J. Schofield, M. Hoesch, C. Meingast, T. Wolf, and A. I. Coldea, *Phys. Rev. B* **91**, 155106 (2015).
- [23] M. D. Watson, T. Yamashita, S. Kasahara, W. Knafo, M. Nardone, J. Béard, F. Hardy, A. McCollam, A. Narayanan, S. F. Blake, T. Wolf, A. A. Haghighirad, C. Meingast, A. J. Schofield, H. v. Löhneysen, Y. Matsuda, A. I. Coldea, and T. Shibauchi, *Phys. Rev. Lett.* **115**, 027006 (2015).
- [24] S. Tan, Y. Zhang, M. Xia, Z. Ye, F. Chen, X. Xie, R. Peng, D. Xu, H. X. Qin Fan, J. Jiang, T. Zhang, X. Lai, T. Xiang, J. Hu, B. Xie, and D. Feng, *Nat. Mater.* **12**, 634 (2013).
- [25] T. Shimojima, Y. Suzuki, T. Sonobe, A. Nakamura, M. Sakano, J. Omachi, K. Yoshioka, M. Kuwata-Gonokami, K. Ono, H. Kumigashira, A. E. Böhmer, F. Hardy, T. Wolf, C. Meingast, H. v. Löhneysen, H. Ikeda, and K. Ishizaka, *Phys. Rev. B* **90**, 121111 (2014).
- [26] K. Nakayama, Y. Miyata, G. N. Phan, T. Sato, Y. Tanabe, T. Urata, K. Tanigaki, and T. Takahashi, *Phys. Rev. Lett.* **113**, 237001 (2014).
- [27] S. Kasahara, T. Watashige, T. Hanaguri, Y. Kohsaka, T. Yamashita, Y. Shimoyama, Y. Mizukami, R. Endo, H. Ikeda, K. Aoyama, T. Terashima, S. Uji, T. Wolf, H. von Löhneysen, T. Shibauchi, and Y. Matsuda, *Proc. Natl. Acad. Sci. U. S. A.* **111**, 16309 (2014).
- [28] T. Terashima, N. Kikugawa, A. Kiswandhi, D. Graf, E.-S. Choi, J. S. Brooks, S. Kasahara, T. Watashige, Y. Matsuda, T. Shibauchi, T. Wolf, A. E. Böhmer, F. Hardy, C. Meingast, H. v. Löhneysen, and S. Uji, *Phys. Rev. B* **93**, 094505 (2016).
- [29] T. Terashima, N. Kikugawa, S. Kasahara, T. Watashige, Y. Matsuda, T. Shibauchi, and S. Uji, *Phys. Rev. B* **93**, 180503 (2016).
- [30] E. Ohmichi and T. Osada, *Rev. Sci. Instrum.* **73**, 3022 (2002).
- [31] P. Blaha, K. Schwarz, G. K. H. Madsen, D. Kvasnicka, and J. Luitz, *WIEN2K*, edited by K. Schwarz (Technische Universität Wien, Austria, 2001).
- [32] We used the PBE-GGA exchange-correlation functional given in J. P. Perdew, K. Burke, and M. Ernzerhof, *Phys. Rev. Lett.* **77**, 3865 (1996), and set $R_{MTK_{max}} = 7.0$ and $8 \times 8 \times 6$ k -mesh in the Brillouin zone.
- [33] M. Decroux and Ø. Fischer, in *Superconductivity in Ternary Compounds II*, edited by M. B. Maple and Ø. Fischer (Springer-Verlag, Berlin, 1982).
- [34] J.-Y. Lin, Y. S. Hsieh, D. A. Chareev, A. N. Vasiliev, Y. Parsons, and H. D. Yang, *Phys. Rev. B* **84**, 220507 (2011).

- [35] D. Shoenberg, *Magnetic oscillations in metals* (Cambridge University Press, Cambridge, 1984).
- [36] K. Yamaji, J. Phys. Soc. Jpn. **58**, 1520 (1989).
- [37] A. Subedi, L. Zhang, D. J. Singh, and M. H. Du, Phys. Rev. B **78**, 134514 (2008).
- [38] A. I. Coldea, J. D. Fletcher, A. Carrington, J. G. Analytis, A. F. Bangura, J.-H. Chu, A. S. Erickson, I. R. Fisher, N. E. Hussey, and R. D. McDonald, Phys. Rev. Lett. **101**, 216402 (2008).
- [39] J. G. Analytis, C. M. J. Andrew, A. I. Coldea, A. McCollam, J.-H. Chu, R. D. McDonald, I. R. Fisher, and A. Carrington, Phys. Rev. Lett. **103**, 076401 (2009).
- [40] H. Shishido, A. F. Bangura, A. I. Coldea, S. Tonegawa, K. Hashimoto, S. Kasahara, P. M. C. Rourke, H. Ikeda, T. Terashima, R. Settai, Y. Ōnuki, D. Vignolles, C. Proust, B. Vignolle, A. McCollam, Y. Matsuda, T. Shibauchi, and A. Carrington, Phys. Rev. Lett. **104**, 057008 (2010).
- [41] J. G. Analytis, J.-H. Chu, R. D. McDonald, S. C. Riggs, and I. R. Fisher, Phys. Rev. Lett. **105**, 207004 (2010).
- [42] T. Terashima, N. Kurita, M. Tomita, K. Kihou, C. H. Lee, Y. Tomioka, T. Ito, A. Iyo, H. Eisaki, T. Liang, M. Nakajima, S. Ishida, S. Uchida, H. Harima, and S. Uji, Phys. Rev. Lett. **107**, 176402 (2011).
- [43] C. Putzke, A. I. Coldea, I. Guillaumon, D. Vignolles, A. McCollam, D. LeBoeuf, M. D. Watson, I. I. Mazin, S. Kasahara, T. Terashima, T. Shibauchi, Y. Matsuda, and A. Carrington, Phys. Rev. Lett. **108**, 047002 (2012).
- [44] M. Yi, D. H. Lu, J. G. Analytis, J.-H. Chu, S.-K. Mo, R.-H. He, R. G. Moore, X. J. Zhou, G. F. Chen, J. L. Luo, N. L. Wang, Z. Hussain, D. J. Singh, I. R. Fisher, and Z.-X. Shen, Phys. Rev. B **80**, 024515 (2009).